Electronic Supplementary Material (ESI) for RSC Advances.

Supporting Information

Ni-P/C electro-catalyst with improved activity for carbohydrazide oxidation reaction

Xinyue Cao†, Haining Wang†, Shanfu Lu*, Sian Chen, Yan Xiang*

Beijing Key Laboratory of Bio-inspired Energy Materials and Devices, School of Space and Environment,

Beihang University, Beijing 100191, PR China.

*Corresponding authors: lusf@buaa.edu.cn, xiangy@buaa.edu.cn

† Equal contribution.

Experimental Section

Catalyst preparation

A two-step route was adopted to fabricate carbon-supported crystalline Ni-P nanoparticles (NPs). Firstly, carbon black supported nickel nanocrystals (Ni/C) were prepared. 0.64 g carbon black (Vulcan® XC-72, Cabot, American) and 1.78 g $NiCl_2 \cdot 6H_2O$ (Beijing Chemical Factory) were totally distributed in 100.0 mL ethylene glycol (Beijing Chemical Factory), and the mixture was kept in a water bath at 65℃ under constant mechanical stirring (600 rpm). Afterwards, 16.0 mL hydrous hydrazine (85 wt %) was dropped into the mixture with constant pressure funnel at a flow rate about 1mL min^{-1}. Then 20.0 mL 10 M KOH solution was added into the mixture, and the Ni/C NPs were obtained after further stirring for another 15 min. The samples were centrifuged and washed with ethanol and deionized water for several times and dried at 50℃ for 2 h in a vacuum drier. After then, 0.193 g Ni/C NPs were distributed in 30 mL ethylene glycol. After sonicating for 30 min, 1.4784 g NaH_2PO_2 (99.9%) was added and mixed in the mixture. The mole ratio of P and Ni sources was changed to synthesize Ni-P/C NPs with different mole ratios (P/Ni=0, 7.0, 9.6, 14.4), which were marked as Ni/C, $Ni_{100}P_{7.0}$/C, $Ni_{100}P_{9.6}$/C, $Ni_{100}P_{14.4}$/C. The final solution was sealed in Teflon-lined stainless steel autoclaves at 180℃ for 3 h, and cooled at room temperature naturally. After being centrifuged (8000 rpm) and washed by ethanol and deionized water for several times, the received catalysts was dried at 50℃ for 2 h in a vacuum drier.

Characterization

Powder X-Ray diffraction (XRD) was performed at room temperature using a Bruker D8 Advance diffractometer with Cu Kα radiation. The XRD profile was recorded at a scan rate of 5° min^{-1} for 2θ values between 10° and 80°. The particle sizes of the Ni/C NPs and Ni-P/C NPs were collected with a scan speed of 2° min^{-1} for 2θ values between 10° and 80°.

The morphology of as-prepared products was characterized by transmission electron microscopy (TEM). The TEM images and selected area electron diffraction (SAED) were collected using a Tecnai G2 F20 S-TWIN microscope at an accelerating voltage of 200 kV. TEM samples were sonicated in alcohol and dropped onto a carbon-coated copper grid. The dot-mapping images were investigated by FEI Titan G2 80-200 transmission electron microscopy operating at 200 KV.

The element compositions and valence states of the Ni/C NPs and Ni-P/C NPs catalysts were probed by X-ray photoelectron spectra (XPS) using a Thermo Scientific Escalab 250Xi spectrometer with an Al Kα (1486.6 eV) radiator.

Electrochemical measurements

The electrochemical measurements were operated in a standard three-electrode system. All electrochemical tests were performed with a CHI760E instrument (Shanghai Chen Hua Instrument Co. Ltd.) and a rotating disk electrode (RDE, Pine Instrument, AFMSRCE). A Pt wire was used as the counter electrode. The working electrode was a glass carbon electrode (GCE, 5 mm in diameter) and the reference electrode was a reversible hydrogen electrode (RHE, pH=14). All potentials throughout this paper were referred to RHE.

5 mg catalyst was dispersed in 1 mL 0.05 wt% Nafion-alcohol solution and sonicated for 20 min to form the catalyst ink. Then 5 μL of the ink is loaded onto the GCE surface and dried using an infrared lamp. The GCE, which was deposited a thin layer of Nafion-bonded catalyst, served as the working electrode.

1.0 M KOH solution were used as electrolytes and was bubbled with nitrogen for 30 min before all the electrochemical tests. Linear sweep voltammetry (LSV) was carried out in a deaerated 1.0 M KOH + 0.1 M carbohydrazide solution at a scan rate of 10 mV s^{-1} to evaluate the catalyst activity for carbohydrazide oxidation reaction. And the cyclic voltammetry (CV) test was conducted at a scan rate of 50 mV s^{-1}. Chronoamperometry (CA) test and electrochemical impedance spectroscopy (EIS) were collected in a nitrogen saturated 1.0 M KOH + 0.1 M carbohydrazide solution at 0.4 V (*vs*. RHE). All tests were carried out at room temperature and maintained under nitrogen atmosphere. The rotation speed of RDE was set to 900 rpm.

Electrochemically active surface area measurement

The electrochemically active surface area of Ni/C and Ni-P/C was measured using the method as reported in reference[1-3]. In our test, the catalysts were activated in the solutions by evolving hydrogen gas at -0.6 V (*vs*. RHE) for 30 min in 1.0 M KOH solution and followed by keeping the potential at 0.05 V (*vs.* RHE). Then CVs was measured from 0.1 to 0.8 V (*vs.* RHE) to obtain the nickel oxidation and reduction characteristics from which the electroactive surface area is determine. The CVs are shown in Fig. S3 and the results of electrochemically active surface areas are presented in Table S1, where $\triangle Q$ is the charge difference of the first and last scan of CV curves and S is the specific surface area. The current density of Ni/C and Ni-P/C NPs was calculated by electrochemically active surface areas.

Theoretical calculation

The geometries and electronic property of Ni-P/C were studied by Density Functional Theory (DFT) calculations using VASP program[4-7]. The surfaces of Ni(111) was modeled using 3-layer slab and 3×3 supercell constructed with lattice bulk constants. Atoms at the bottom layer were fixed and all other atoms were allowed to relax in any directions during geometry optimization. The varied P ratio is represented by using different number of P atoms at the top layer. A vacuum layer of about 12 Å was used to eliminate the interaction between periodic slabs. The projector-augmented wave (PAW) formalism implementing the generalized gradient approximation as parameterized by Perdew et al. (PBE)[8] was used. The plan-wave kinetic energy cutoff is used as 300 eV, and the k-points meshes were set as 6×6×1. All structures were fully relaxed until the convergence in energy and force reached 1.0×10^{-5} eV and 1.0×10^{-4} eV/Å. The convergence tests revealed all these parameters were sufficient. The optimized structure is shown in Fig. S4.

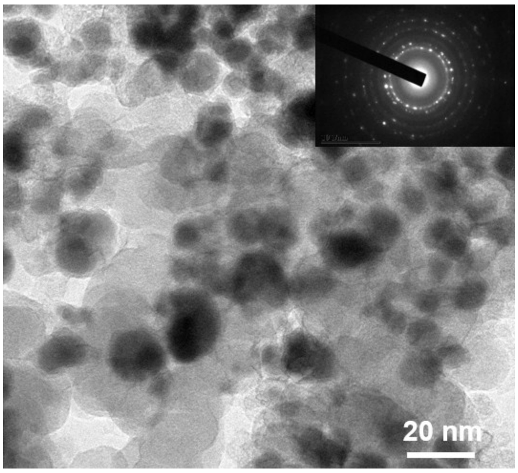

Fig. S1 TEM image and SAED image (inset) of Ni/C NPs.

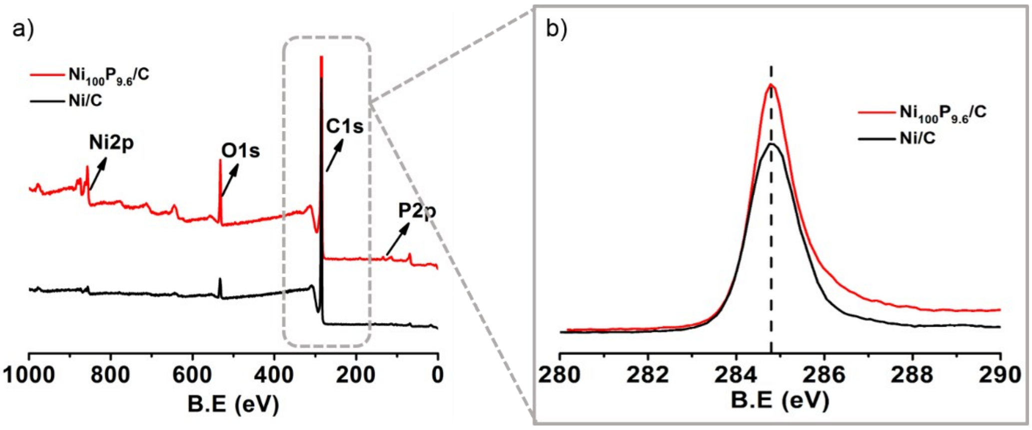

Fig. S2 (a) Full XPS spectra and (b) C 1s orbital binding energy regions of Ni/C and Ni-P/C NPs.

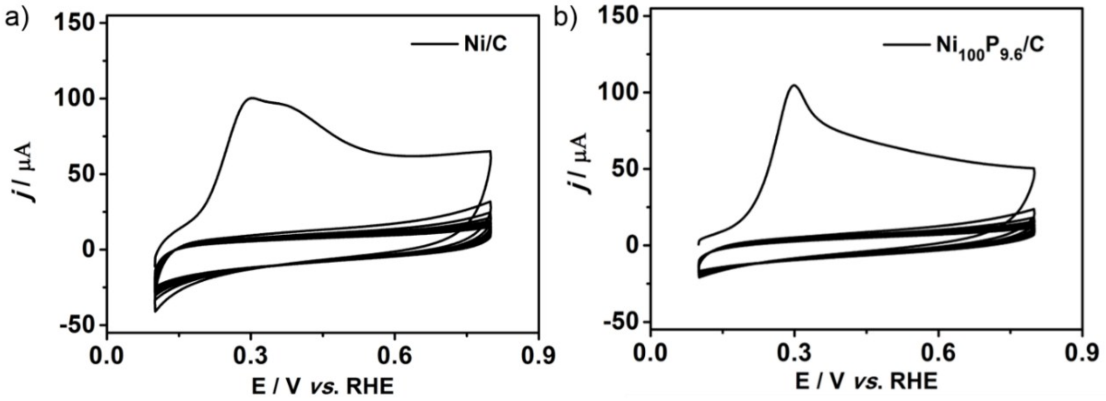

Fig. S3 CV curves of a) Ni/C NPs and b) Ni-P/C NPs in 1.0 M KOH + 0.1M carbohydrazide solution.

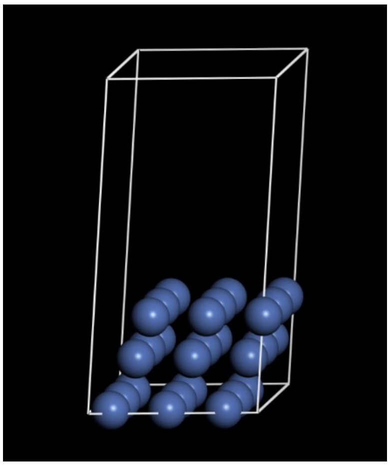

Fig. S4 The optimized structure of Ni NPs

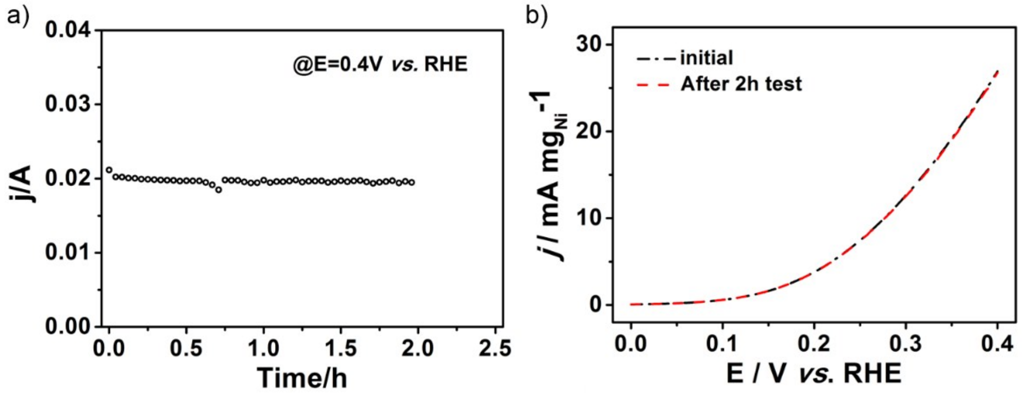

Fig. S5 (a) The Current-time curves at 0.4 V (vs. RHE) for 2h and (b) LSV curves before and after durability test of Ni-P/C for carbohydrazide oxidation reaction. Test conditions: Ni-P/C 15 mg/cm^2, electrode area 1 cm^2, 1.0 M KOH + 0.1 M carbohydrazide solution, room temperature.

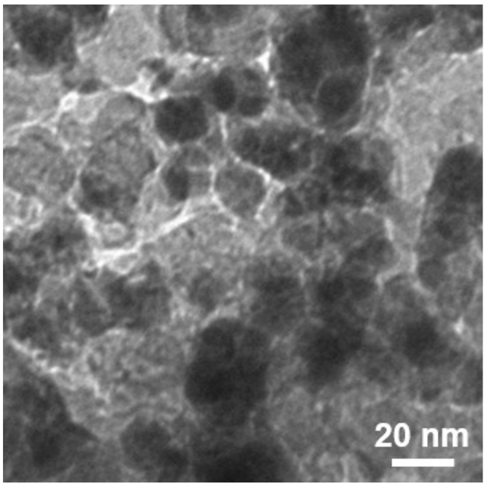

Fig. S6 TEM image of Ni–P/C NPs after durability test of 2h.

Table S1 Electrochemically active surface area measurement of Ni/C and Ni–P/C NPs.

Material	△Q (C)	S (m^2/g)	Current density (mA cm^{-2}) @0.4V (*vs.* RHE)
Ni/C	9.90E-4	7.616	0.013
$Ni_{100}P_{9.6}/C$	8.95E-4	6.884	0.211

Table S2 The charge of each Ni atoms in Ni-P particles with varied Ni:P ratio at the top layer in comparison with that in Ni particle. The charge was obtained using Bader charge analysis from DFT calculation.

	Ni_7P_2	Ni_4P_5	Ni_1P_8
Charge [e]	+0.04	+0.17	+0.20

Reference

1 V. Ganesh and V. Lakshminarayanan, *Electrochim. Acta*, 2004, **49**, 3561-3572.

2 I. J. Brown and S. Sotiropoulos, *Electrochim. Acta*, 2001, **46**, 2711-2720.

3 I. J. Brown and S. Sotiropoulos, *J. Appl. Electrochem.*, 2000, **30**, 107-111.

4 G. Kresse and J. Hafner, *Phys. Rev. B*, 1993, **47**, 558-561.

5 G. Kresse and J. Hafner, *Phys. Rev. B*, 1994, **49**, 14251-14269.

6 G. Kresse and J. Furthmüller, *Comput. Mater. Sci.*, 1996, **6**, 15-50.

7 G. Kresse and J. Furthmüller, *Phys. Rev. B*, 1996, **54**, 11169-11186.

8 J. P. Perdew, K. Burke and M. Ernzerhof, *Phys. Rev. Lett.*, 1996, **77**, 3865-3868.